Discovery of a novel Mycobacterial F-ATP synthase inhibitor and its potency in combination with diarylquinolines

Adam Hotra[1,2,3], Priya Ragunathan[2], Pearly Shuyi Ng[4], Pattarakiat Seankongsuk[1], Amaravadhi Harikishore[1,2], Jickky Palmae Sarathy[5], Wuan-Geok Saw[2], Umayal Lakshmanan[4], Patcharaporn Sae-Lao[1], Nitin Pal Kalia[6], Joon Shin[2], Revathy Kalyanasundaram[7], Sivaraj Anbarasu[7], Krupakar Parthasarathy[7], Chaudhari Namrata Pradeep[2], Harshyaa Makhija[2], Peter Dröge[2], Anders Poulsen[4], Jocelyn Hui Ling Tan[4], Kevin Pethe[2,6], Thomas Dick[5,8,9], Roderick W. Bates[1,*], and Gerhard Grüber[2,*]

Abstract: The F_1F_O-ATP synthase is required for growth and viability of *Mycobacterium tuberculosis*. Bedaquiline validated this target clinically. We showed recently that a mycobacterium-specific loop of the enzyme's rotary γ subunit plays a role in coupling of ATP synthesis within the enzyme complex. Here, we report the discovery of a novel antimycobacterial, termed GaMF1, targeting this γ subunit loop. Biochemical and Nuclear Magnetic Resonance studies show that GaMF1 inhibits ATP synthase activity by binding to the loop. GaMF1 is bactericidal and is active against multidrug- as well as Bedaquiline-resistant strains. Chemistry efforts on the scaffold revealed a dynamic structure activity relationship and delivered analogues with nanomolar potencies. Combining GaMF1 with bedaquiline or novel diarylquinoline analogues showed potentiation without inducing genotoxicity or phenotypic changes in a human embryonic stem cell reporter assay. These results suggest that GaMF1 presents an attractive lead for the discovery of a novel class of anti-tuberculosis F-ATP synthase inhibitors.

[1]School of Physical and Mathematical Sciences, Nanyang Technological University, 21 Nanyang Link, Singapore 637371, Republic of Singapore; E-mail: roderick@ntu.edu.sg
[2]School of Biological Sciences, Nanyang Technological University, 60 Nanyang Drive, Singapore 637551, Republic of Singapore; E-mail: ggrueber@ntu.edu.sg
[3]Nanyang Institute of Technology in Health and Medicine, Interdisciplinary Graduate School, Nanyang Technological University, Republic of Singapore
[4]Experimental Drug Development Centre, Agency for Science Technology and Research, A*STAR, 10 Biopolis Road, Singapore 138670
[5]Department of Microbiology and Immunology, Yong Loo Lin School of Medicine, National University of Singapore, 14 Medical Drive, Singapore 117599, Republic of Singapore
[6]Lee Kong Chian School of Medicine, Nanyang Technological University, Experimental Medicine Building, Singapore
[7]Centre for Drug Discovery and Development, Sathyabama Institute of Science and Technology, Chennai 600119, India
[8]Center for Discovery and Innovation, Hackensack Meridian Health, 340 Kingsland Street, Nutley, NJ 07110, USA
[9]Center for Discovery and Innovation, Hackensack Meridian Health, 340 Kingsland Street, Nutley, NJ 07110, USA

Introduction

Tuberculosis (TB) is a devastating disease that results in 1.4 million deaths every year.[1] Multidrug resistant- (MDR) and extensively drug-resistant (XDR) bacterial strains of *Mycobacterium tuberculosis* (*Mtb*), which causes TB, are spreading worldwide, causing major global health issues. Furthermore, about one third of the world population is latently infected by Koch's bacillus and susceptible to develop the disease.[1] During infection, *Mtb* inhabits a wide range of intracellular and extracellular environments. Many of these environments are highly dynamic, and mycobacteria face with the constant challenge of redirecting their metabolic activity commensurate with either growth or non-replicating persistence.[2] A fundamental feature in this adaptation is the ability of mycobacteria to respire, regenerate reducing equivalents, and generate the biological energy currency adenosine triphosphate (ATP) via oxidative phosphorylation. During the latter, an electrochemical gradient of protons is generated by the electron transport chain (ETC; Fig. 1A). The electrochemical gradient drives the energy converter F_1F_O ATP synthase and is required for viability of growing and non-growing mycobacteria.[2] Phenotypic screening identified the first-in-class diarylquinoline drug bedaquiline (BDQ, Sirturo®) that inhibits the mycobacterial F-ATP synthase (Fig. 1A-B).[3] However, the successful advance of this drug has been overshadowed by the development of clinical resistance [4] along with a very long terminal half-life leading to concerns regarding tissue accumulation.[5] Recent medicinal chemistry campaigns resulted in a new generation of 3,5-dialkoxypyridine (DARQ) analogues of BDQ that have the potential to address these issues.[6] TBAJ-587 and -876 are new development compounds of this series (Fig. 1B), showing improved physio-chemical properties.[6] The discovery of squaramides (SQA) [7], compound 5228485 [8], and epigallocatechin gallate (EGCG) [9] as potent ATP synthesis inhibitors underlined the relevance of the mycobacterial F-ATP synthase as a drug target.

Nevertheless, infections with MDR- and XDR *Mtb* strains and coinfection with HIV have worsened the prospect of controlling TB.[10] In addition, the prolonged treatment regimen for six months with a combination of four drugs has resulted in poor patient compliance, leading to the emergence of MDR and XDR strains of *Mtb.*[11] Therefore, in order to improve the effectiveness of TB treatment and to improve control of MDR and XDR TB, new antitubercular targets and agents are required. Anti-TB targets should be a) essential for viability in *Mtb*, b) novel to avoid of cross resistance with existing drugs, c) absent in humans to avoid mechanism-based toxicity issues.

The F_1F_O ATP synthase is essential for growth and viability in mycobacteria.[12] In contrast, in other prokaryotes, the enzyme is dispensable for growth on fermentable carbon sources.[13] The mycobacterial enzyme is composed of a membrane-embedded F_O complex (subunits *a*:*b*:*b'*:c_9), responsible for H^+-translocation from the periplasmic space to the cytoplasmic side, and the F_1 part (subunits α_3:β_3:γ:ε) [14] which uses the proton-motive force to synthesize ATP within the three catalytic αβ-pairs (Fig. 1A). This catalytic $\alpha_3\beta_3$-headpiece is linked with the F_O part via the two rotating central stalk subunits γ and ε, as well as the peripheral stalk subunits *b*, *b'* and δ.[14c, 14e].

We recently demonstrated the specific role of the unique loop of mycobacterial subunit γ (γ166-179-loop; *M. smegmatis*

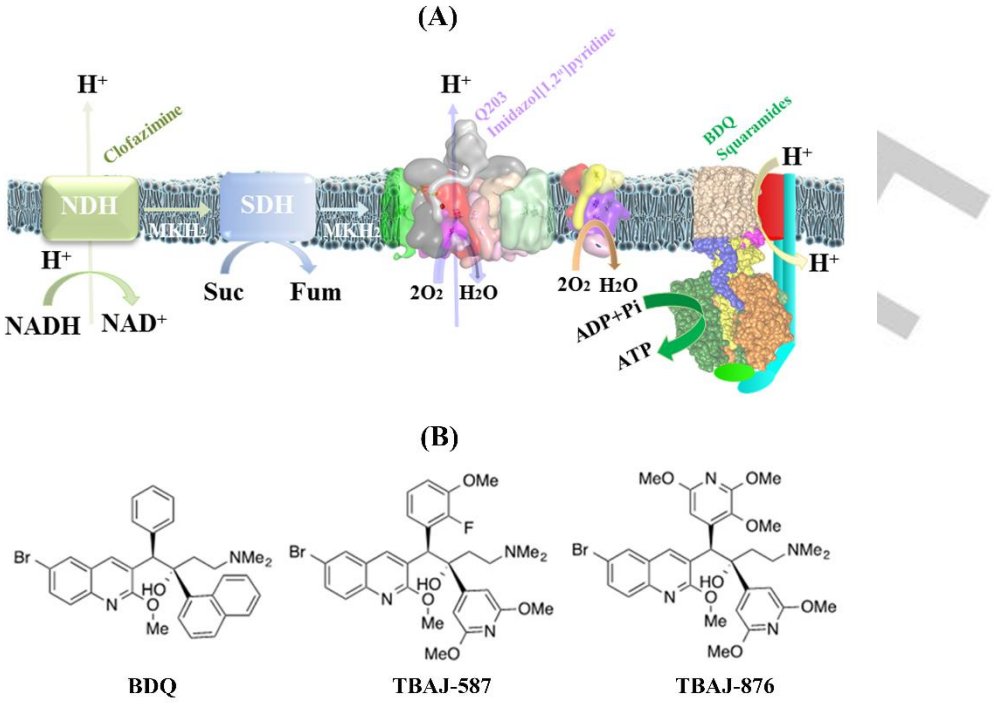

Figure 1. (*A*) Enzyme composition and inhibitors of the electron transport chain and F-ATP synthase of *Mtb*. (*B*) Structures of BDQ, TBAJ-587 and TBAJ-876.

numbering) effecting ATP hydrolysis, -driven H^+-pumping and -synthesis.[15] As the mycobacterial γ-loop is unique, absent in the human homologue and other prokaryotes, as well as important for the regulation of ATP synthesis, -hydrolysis and proton pumping, it fulfils fundamental criteria as a potential TB-drug target.

We here conducted an *in silico* compound screening exercise based on our structural and biochemical data of the mycobacterial enzyme F-ATP synthase [15, 16] that led to the discovery of the mycobacterial F-ATP synthase inhibitor GaMF1. The variety of biochemical assays, the use of a BDQ-resistant F-ATP synthase mutant and structural experiments validated that GaMF1 exerts its anti-mycobacterial activity through inhibition of the F-ATP synthase. Furthermore, GaMF1 increased the potency of BDQ and other DARQ analogues, opening a new avenue for an efficient multi-drug combination. In addition, initial structure-activity relationship studies (SAR) revealed a path to optimize the potency of the series.

Results and Discussion

Homology and Pharmacophore Modelling

The γ166-179 loop was exploited as a binding epitope for *de novo* drug design. [15, 16] As high-resolution crystallographic structures were lacking when the project started, homology

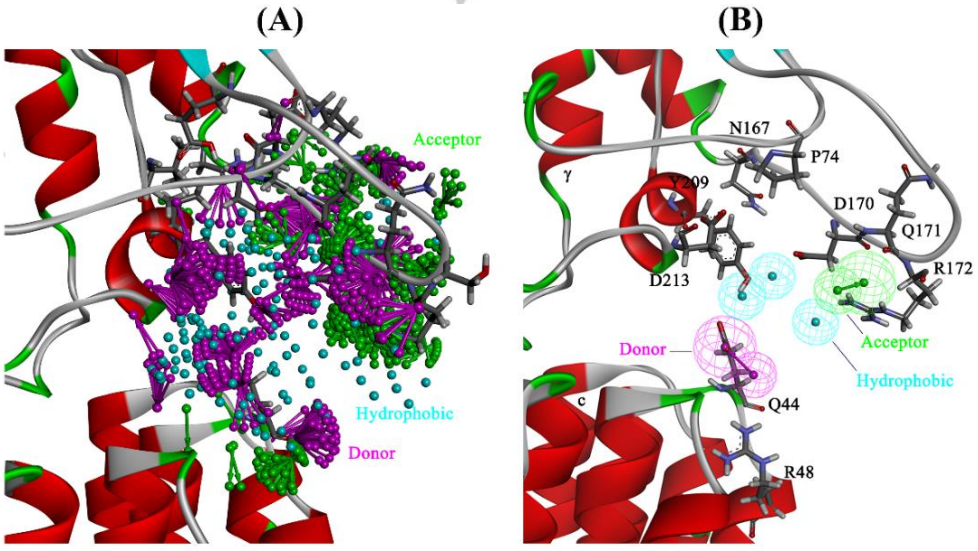

Figure 2. Receptor-based pharmacophore modeling and pharmacophore mapping. (*A*) Generation of Ludi-based interaction sites using acceptor, donor, and hydrophobic features as probes at γ166-179 loop-*c* ring interface residues. (*B*) Five features comprising of one hydrogen bond acceptor (*green sphered arrows*) in vicinity of R172 sidechain atoms, one hydrogen bond donor targeting Q44 residue of the c-ring (*magenta sphered arrows*), three hydrophobic features (*cyan spheres*) in the vicinity of P74, Y209, R172 residues were included in the receptor based pharmacophore model.

modelling enabled us to build 3D structures with good accuracy (see Supplementary Information). Our receptor-based pharmacophore modelling studies highlighted the possible interaction sites at the γ166-179 loop interface (Fig. 2A). Mainly, one hydrogen bond acceptor, one hydrogen bond donor and three hydrophobic features were included in the pharmacophore model at the γ166-179 loop-*c* ring interface (Fig. 2B). Further, the exclusion volumes constraints around protein atoms near the ligand (not shown for clarity) were also incorporated to delineate the shape of the binding cavity as well as to prevent clashes of ligand with protein atoms. Database screening with a 5-feature mapping resulted in library of about 30,000 molecules. This library was further refined by a series of standard precision, extra precision docking protocols with glide score, XP scores and consensus scoring themes. Together with visual inspection of molecular interactions at the γ166-179 loop and *c*-ring interface resulted in 81 molecules for experimental screening.

Antimycobacterial activity and Minimum inhibitory concentration determination

We identified ligands that bear complementarity to the γ166-179 loop and *c*-ring interface and provided a focused library of which GaMF1 (Fig. 3A) exhibited a minimal inhibitory concentration (MIC_{50}) of 11 µM in the fast growing *M. smegmatis* mc^2 155 strain, 17 µM in *M. bovis* bacillus Calmette–Guérin (BCG), and 33 µM in *Mtb* H37Rv (Fig. 3B). A synthesis protocol for GaMF1 was established (see Supplementary Information: *Synthesis of GaMF1*) to produce the compound in bulk to study the bactericidal activity of the compound and its mechanism of action. GaMF1 was bactericidal against *M. smegmatis* mc^2 155 at 20-fold its MIC_{50}, indicated by the decreasing cell number of about 99% in 3 days (Fig. 3C) In contrast, BDQ had delayed bactericidal activity, as reported before [17], followed by a reduction in bacterial viability (Fig. 3C). GaMF1 was also bactericidal

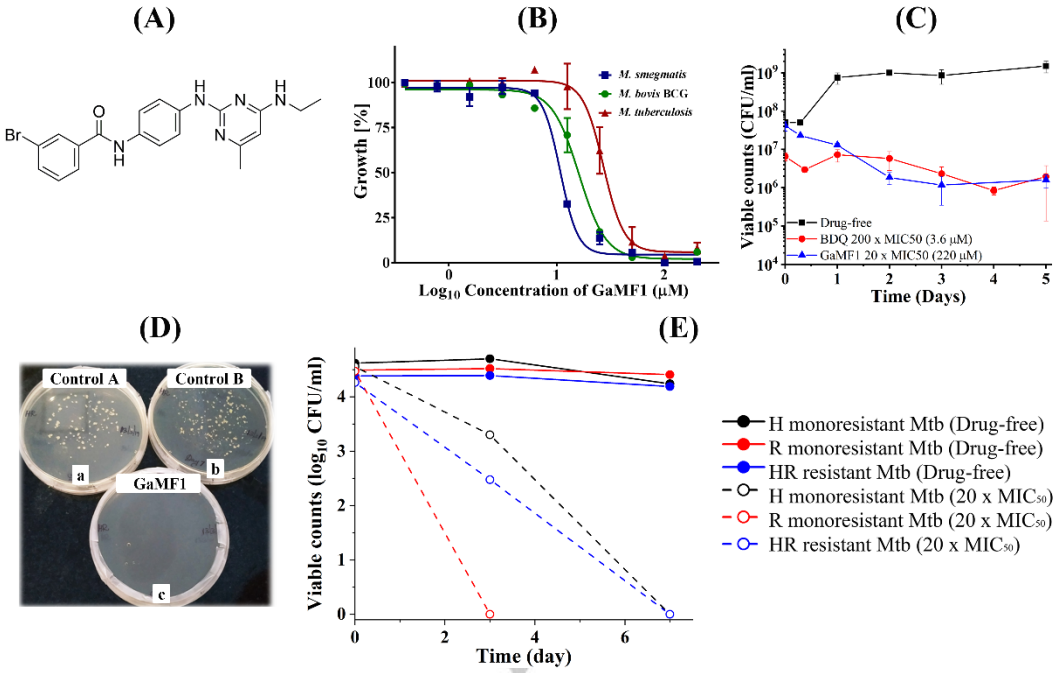

Figure 3: (*A*) Structure of GaMF1. (*B*) Growth inhibition of *M. smegmatis* (*blue*), *M bovis* BCG (*green*) and *Mtb* (*red*) by GaMF1 with MIC_{50} of 11, 17 and 33 µM, respectively. (*C*) Initial five days of GaMF1-, BDQ kill kinetics against *M. smegmatis* mc^2 155. The bacteria were grown in liquid culture (LBT) in the presence of the indicated concentrations of GaMF1 and BDQ. The experiments were repeated twice, and the profiles were identical. (*D*) Images (*a*, *b*), HR resistant *Mtb* colonies observed after day 7 incubation in no-compound containing Middlebrook 7H9 broth (4.188 $\log_{10}$ CFU/ml); Image (*c*), no colonies of HR resistant *Mtb* observed after day 7 incubation in compound GaMF1 containing Middlebrook 7H9 broth. (*E*) Antimycobacterial activity of GaMF1 against *Mtb* isolate resistant to Isoniazid (H) and Rifampicin (R) as determined by Colony forming units (CFU) based method in Middlebrook 7H11 agar plates.

against three drug resistant clinical isolates (isoniazid (H), rifampicin (R) monoresistant- and HR-resistant *Mtb* strains), causing a significant reduction in bacterial viability in 3 to 7 days (Fig. 3D- E). Preliminary *in vitro* ADME profiling revealed that that GaMF1, with a clogP value of 4.37, is less lipophilic than BDQ [6c], and has a good metabolic stability in mouse liver microsomes ($T_{½}$ with or without NADPH of 47.5 min and 68 min, respectively; Cl_{int} of 14.6 µl/min/mg protein (Supplementary Table 1A-B)).

Insights into the inhibition of mycobacterial F-ATP synthase by GaMF1

To confirm that GaMF1 exerts its anti-mycobacterial activity via inhibition of the mycobacterial F-ATP synthase, ATP synthesis was measured using inverted membrane vesicles (IMVs) of *M. smegmatis* and *M. bovis* BCG. Figure 4A shows a typical profile of *M. smegmatis* IMVs ATP synthesis inhibition by BDQ with a half-maximal inhibitory concentration (IC_{50}) of 1.1 ± 0.2 nM, which is in line with previous reports [15, 18], and an IC_{50} of 7.1 ± 1.3 nM *M. bovis* BCG (Fig. 4B). In comparison, GaMF1 revealed a potent ATP synthesis inhibition at an IC_{50} of 0.5 ± 0.1 µM in *M. smegmatis* IMVs (Fig. 4A) and 5.2 ± 1.1 µM in *M. bovis* BCG (Fig. 4B). GaMF1 inhibited ATP synthesis of *M. smegmatis* (Fig. 4A) and *M. bovis* BCG (Fig. 4B) IMVs in the presence of succinate, indicating that GaMF1 does not interfere with the NADH-dehydrogenases. In parallel, a possible effect of GaMF1 on oxygen consumption and thereby the cytochrome oxidases of the ETC was tested using methylene blue as an oxygen probe. As visualized for the fast- and slow grower *M. smegmatis* (Fig. 4C) and *M. bovis* BCG (Fig. 4D), oxygen consumption was unaffected in both strains at µM concentrations of GaMF1. In comparison, nM- and µM concentrations of BDQ revealed a slight and moderate effect on oxygen respiration in both strains (Fig 4C-D), reflecting that BDQ does also affect oxygen consumption as described by Kalia et al. [19]

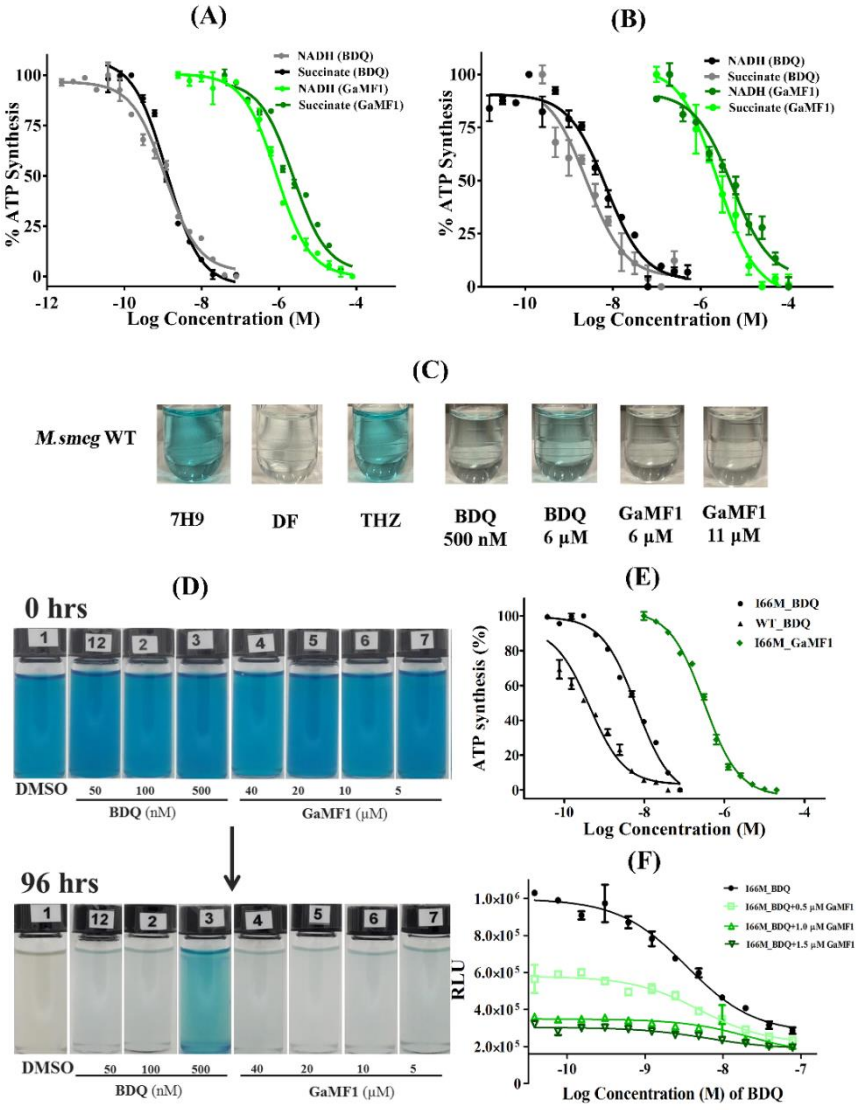

Figure 4: Inhibition of ATP synthesis by GaMF1 in IMVs from *M. smegmatis* (*A*) and *M. bovis* (*B*) using the electron donors NADH (*dark green*) or succinate (*light green*). BDQ was used as a control BDQ (*black/grey*). (*C-D*) Test of possible effects of GaMF1 and BDQ on oxygen consumption in *M. smegmatis* IMVs (*C*) and *M. bovis* BCG cells (*D*). BDQ shows partial inhibition of oxygen consumption at nanomolar range (500 nM) and significant inhibition at micro-molar level (6 µM). In comparison, GaMF1 did not inhibit oxygen consumption even at high micro-molar level (6- or 11 µM). Thioridazine (THZ) was used as positive control and 7H9 media /drug free (DF) served as a blank/negative control (*C*). GaMF1 did also not affect oxygen consumption in the slow grower *M. bovis* over a 96-h period, while BDQ at 500 nM completely inhibited oxygen consumption (*D*). (*E*) Inhibition of ATP synthesis by BDQ (*black*) and GaMF1 (*green*) on *M. smegmatis* I66M *c* subunit mutant IMVs with NADH as substrate. The *M. smegmatis* I66M mutant IMVs (●) reveal a 10-fold sensitivity compared to WT (▲), while the inhibitory profile of GaMF1 on *M. smegmatis* I66M mutant IMVs (♦) did not alter. (*F*) Additive effect of GaMF1 and BDQ (*black*) on the ATP synthesis inhibition in IMV's of *M. smegmatis* I66M mutant. In the I66M mutant, BDQ cannot fully inhibit the ATP synthesis. However, when GaMF1 (*green*) was added in a concentration dependent manner, ATP synthesis significantly decreased to almost full inhibition.

We next tested the potency of GaMF1 against an F-ATP synthase bearing an I66M substitution in the *M. smegmatis* subunit *c*, which is associated with resistance to BDQ. [20] While the mutant displayed a 10-fold shift in sensitivity to BDQ (Fig. 4E), the mutation did not affect the potency of GaMF1 (Fig. 4E). Interestingly, addition of GaMF1 reduced ATP synthesis of the I66M mutant IMVs significantly in a concentration dependent manner (Fig. 4F), demonstrating that the novel F-ATP synthase inhibitor GaMF1 shows no cross resistance to BDQ.

Target specificity of GaMF1

The *in vitro* assay data revealed that GaMF1 inhibits ATP synthesis and the growth of *M. smegmatis* and *M. bovis* BCG strains. Next, we performed NMR titration experiments to assess whether GaMF1 does bind to the *M. tuberculosis* γ166-179 peptide, which according to its NMR solution structure, forms a loop of polar residues with a surface distribution of negatively charged residues on one side and an amphiphilic charge distribution on the other side of the loop.[16] The chemical shift perturbations (CSPs) for NH and Hα between free peptide and the peptide-GaMF1 complex derived from the 2D-TOCSY spectra of the *Mt*γ166-179-loop with GaMF1 suggest that the amino acids N167, G168, E169, R172, and S173 became perturbed upon ligand binding (Fig. 5A-B). The data reflect the involvement of γ166-179-loop residues in GaMF1-binding.

To obtain further insights into the molecular interactions of GaMF1, we docked the ligand into subunit *Mt*γ using the NMR perturbed residues as ambiguous interaction restraints (AIR) or active site residues for ligand docking (Fig. 5C). GaMF1 comprises of a 3-bromo-benzoyl moiety (ring A), a 1,4 diaminobenzene moiety (ring B) and a substituted pyrimidine (ring C) and was predicted to bind to a region in the vicinity of the *Mt*γ-

loop residues with a glide score of 5.58 (and a GOLD PLP fitness of 46.5). Both ring A and -B of GaMF1 are involved in interactions with the γ166-179 loop residues. On one hand, the carbonyl and the amide atoms on ring A were engaged in close contacts with γQ171 side-chain amide atoms and γD64 main-chain amide atoms. On the other hand, the 3-bromo benzene group on ring A was also involved in π-alkyl interactions with amino acids γH65 and alkyl atoms of γ R172 (*highlighted by pink lines*). This moiety is positioned in the vicinity of the *c*-ring residues such as *c*R52, *c*Q46, *c*P47, *c*E48 (*beige coloured*) via close contacts, and thereby chaperone the stability of ligand binding at the *Mt*γ-*c* interface. The phenyl-ring (ring B) and pyrimidine (ring C) of GaMF1 were engaged in π-anion interactions (*orange arrows*) with γE169 and γE70 residues, respectively. The 6-methyl on ring C maintained aliphatic hydrophobic interactions with γI214 (*pink line*, (α2 / β5 loop, *light red*)). In addition, the amide atoms which link the 3-N-ethyl fragment on ring C mediate the hydrogen bonding interactions with γR71 residues from α1/β1 loop (*blue*), while the N-ethyl fragment was engaged in van der Waal's contacts with γP72 (*light green line*) and γD174 residues (Fig. 5C).

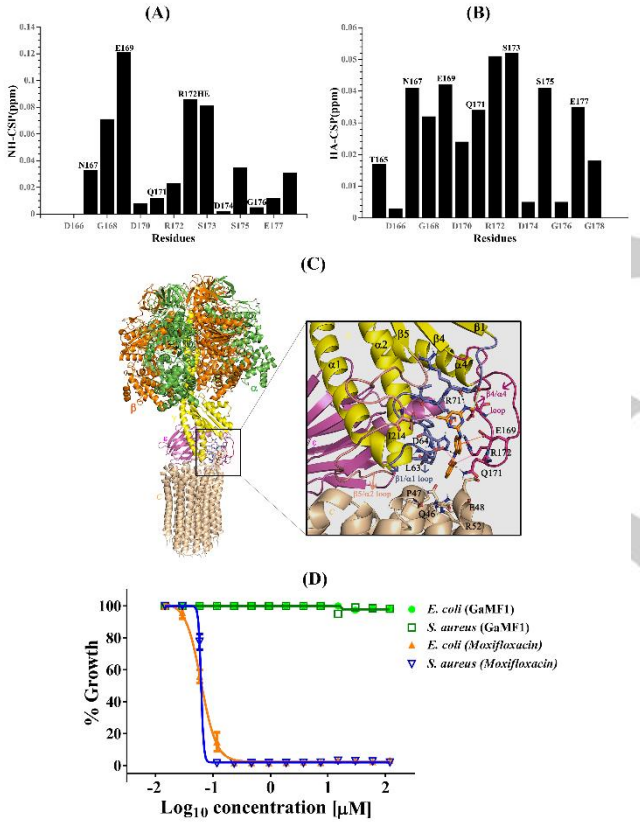

Figure 5: (*A*) 2D-TOCSY NMR spectral data of the free *Mtb* γ166-179 peptide and complexed with GaMF1 highlights the chemical shift changes for NH resonances (absolute values of CSP) between free and complex peptide. (*B*) Absolute values of CSP for HA resonances between free and the GaMF1-bound γ166-179 peptide. (*C*) Predicted binding interaction of GaMF1 on the mycobacterial γ-c ring interface. The three loop regions of β1/α1 (*blue*), β5/α2 (*light red*) and β4/α4 (*magenta*) and together with residues of the *c*-ring loops (*beige*) form the ligand binding pocket. (*D*) A screen of GaMF1 against *S. aureus* and *E. coli*, as representatives of the human microbiome, confirm the specificity of GaMF1 for *Mtb* as well as that the compound does not affect the human microbiome.

To confirm its target specificity and to demonstrate that GaMF1 is not a broad spectrum antibiotic, the compound was tested against *Staphylococcus aureus* and *Escherichia coli* as representatives of Gram-positive and Gram-negative bacteria, respectively (Fig. 5D). While the antibiotic Moxiflocaxin, which is active against both Gram-positive and Gram-negative bacteria by inhibiting DNA gyrase, inhibits both the growth of *S. aureus* and *E. coli*, no growth inhibition of the two bacteria strains was observed in the presence of increasing concentration of GaMF1. Since the extra γ-loop is specific to mycobacterial F-ATP synthases, GaMF1 is not expected to bind to the *E. coli* or *S. aureus* F-ATP synthase and consequently should not inhibit the major energy converter of these prokaryotic cells. NMR titration experiments and docking studies are consistent with a direct interaction between GaMF1 and the subunit *Mt*γ. However, we cannot exclude the possibility that GaMF1 may interfere with additional targets in the pathogen. Future studies could focus on the selection of escape mutants resistant to GaMF1 to confirm target engagement genetically, or alternatively to identify indirect mechanism of resistance such as those described for BDQ of clofazimine [21].

GaMF1 synergizes with BDQ and TBAJ-876 analogs

The *in vitro* ATP synthesis experiments of the I66M mutant IMVs and GaMF1 indicated a synergistic effect but no cross resistance to the diarylquinoline BDQ (Fig. 4F). To assess a synergistic effect of both compounds in more detail, the effect of drug combinations on the growth inhibition of *M. smegmatis* was examined. BDQ inhibited growth at 31.3 nM. However, in combination with GaMF1, the IC_{50} of BDQ reduced with the concentration of GaMF1 added, thus confirming a synergistic effect of both compounds (Fig. 6A). Next, the synergistic effect on ATP synthesis was studied in *M. bovis* BCG. In the whole cell ATP synthesis assay, an additive effect of BDQ and GaMF1 was observed (Fig. 6B). BDQ alone at 200 nM reduced ATP synthesis from $3.7x10^4$ RLU to $8x10^3$ RLU. After addition of GaMF1, ATP formation dropped in a concentration dependent manner of GaMF1 and lowered the IC_{50} of BDQ significantly (Fig. 6B).

Most recently, diarylquinoline analogs with improved potency and physio-chemical properties have been described. [6a-6c] These improved analogues include 5307, 5316, and 5377 [6c] that interact with the subunit *c*-ring and subunit ε of the mycobacterial F-ATP synthase [6d] (Fig. 6C). Using a modified synthesis protocol (see Supplementary *Information*) the racemates of 5307 ((±)-5307), 5316 ((±)-5316), and 5366 ((±)-5366) were synthesized (CCDC deposition numbers: 1967685, 1967683, 1967684, respectively), which inhibited *M. smegmatis* mc^2 155 growth at an MIC_{50} of 1.6 nM, 4.4 nM and 1.0 nM, respectively (Fig. 6D). The improved MIC_{50} values of the racemates compared to BDQ were in line with improved IC_{50} in ATP synthesis inhibition of *M. smegmatis* mc^2 155 IMVs with values of 0.1 ± 0.01 nM, 0.2 ± 0.08 nM, and 0.6 ± 0.33 nM for the racemates 5307, 5316, and 5366, respectively (Fig. 6E). Importantly, combining (±)-5307 with 300 nM of GaMF1 revealed a significant reduction in cell growth (Fig. 6F), demonstrating that the potency of the already improved DARQ derivative increased by the synergistic effect of GaMF1. These results open a new avenue for the development of a novel combinatory drug regimen. Interestingly, the combination of 300 nM GaMF1 with either (±)-5316 or (±)-5366 did not cause a synergistic effect, reflecting a specific combinatorial potency of (±)-5307 and GaMF1.

Viability and pluripotency of human embryonic stem cells remain unaffected by BDQ, (±)-5307 and GaMF1

Human stem cell technologies are becoming increasingly important as valuable *ex vivo* test models during the drug discovery process (reviewed in [22]). We therefore decided to employ a human embryonic stem cell (hESC) line (E3) that we have recently genetically engineered into a highly sensitive pluripotency reporter [23], and examined both potential drug-induced genotoxicity and perturbations of the hESC transcriptional program that lead to hESC differentiation. The assays revealed that neither the tested compounds (±)-5307, (±)-

5307 in combination with 300 nM GaMF1 nor the control BDQ elicited substantial genotoxic effects or induced major alterations in the global transcriptional program (Supplementary Information; Supplementary Fig. 2A-G).

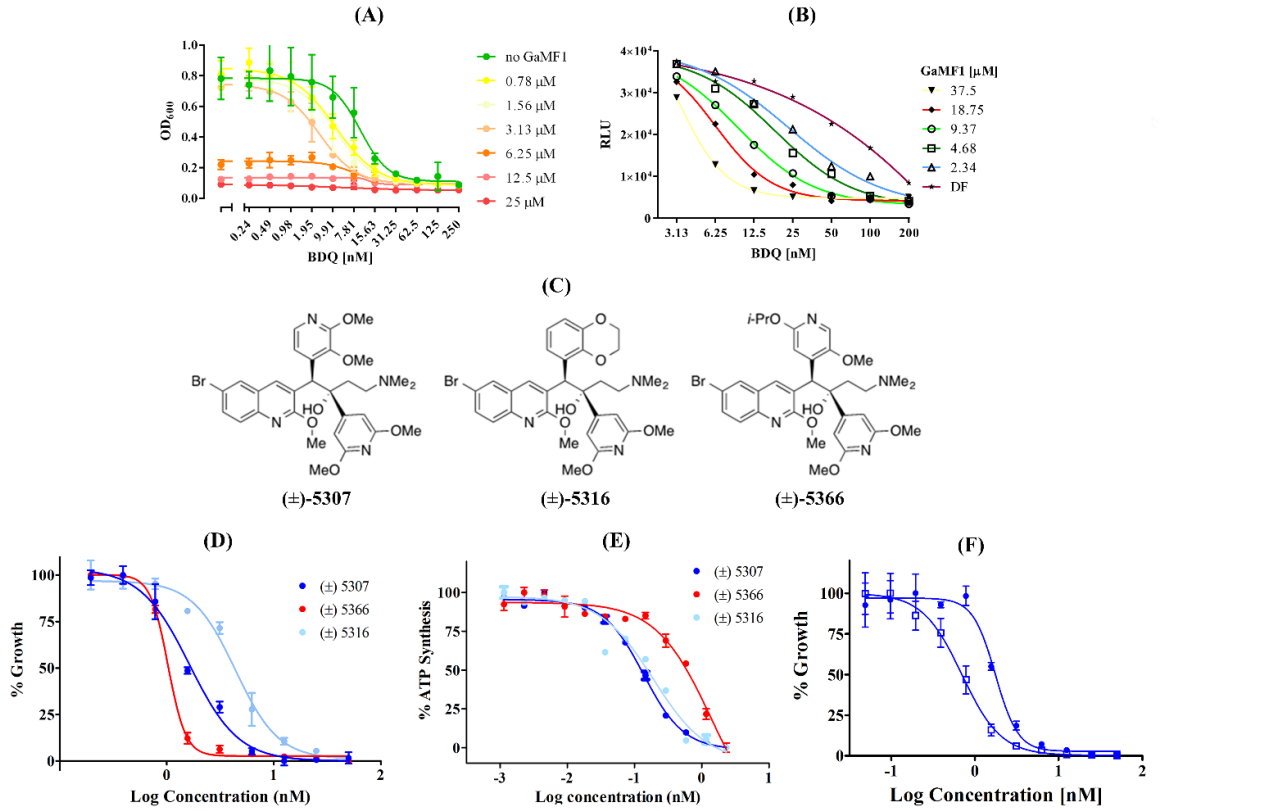

Figure 6: (*A*) Synergistic effect of the TB drug BDQ and GaMF1 on cell growth of *M. smegmatis*. Combination of different concentrations of BDQ and GaMF1 was done by two subsequent serial dilutions in the 96 well plate containing 100 µl of 7H9 media. Suspension of *M. smegmatis* mc^2 155 in logarithmic growth phase was added to obtain starting OD_{600} = 0.05 in 200 µl. Plates were incubated 24 h in 37 °C. (*B*) Whole cell ATP synthesis assay with *M. bovis* BCG in the presence of BDQ and GaMF1. (*C*) Structures of (±)-5307, (±)-5316, and (±)-5366. (*D*) ATP synthesis inhibition of *M. smegmatis* IMVs by (±)-5307, (±)-5316, and (±)-5366, respectively. (*E*) *M. smegmatis* growth inhibition affected by (±)-5307 (●) and in combination with 300 nM of GaMF1 (□).

SAR studies of GaMF1 series

In order to improve the efficacy of GaMF1, a series of analogs was synthesized (see Supplementary Information) and tested in mycobacterial ATP synthesis assay (IC_{50}) and in the mycobacterial assay (*M. smegmatis* and/or *Mtb* MIC_{50}). Key SAR findings are summarized in Table 1.

It was established that ring C was essential for maintaining activity as truncated analog **1** (Table 1) did not inhibit ATP synthesis (IC_{50} > 100 µM). The amide functionality linking rings A and B was essential for activity as switching to the reverse amide **2** led to a loss in activity. This is consistent with the docking pose presented previously (Fig. 5C), where the carbonyl and amide atoms on ring A were predicted to be in close contacts with γQ171 and γD64.

While the removal of substitution on the phenyl ring (**3**) led to a modest drop in activity, replacement of the 3-bromo with either electron-withdrawing CF_3 (**4**) or electron-donating pyrrolidine (**5**) substituents gave compounds with comparable potencies. This result suggests that lipophilic substitutions are preferred in this part of the molecule and that the electronics of the aromatic ring have little contribution towards potency. This observation is also consistent with the docking pose (Fig. 5C), which shows (i) space to tolerate substituents on the phenyl ring and (ii) no key interactions between the neighbouring residues and the phenyl ring. Hence, we concluded that the region around phenyl ring A would perhaps be the most amendable to structural modifications.

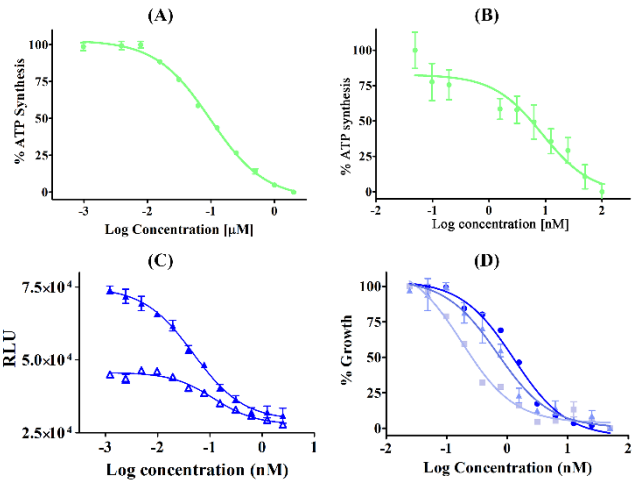

Figure 7: Inhibition of ATP synthesis by GaMF1 analog **8** in IMVs from *M. smegmatis* with an IC_{50} of 90 nM on *M. smegmatis* (*A*) and 8.7 nM on *M. bovis* BCG IMVs (*B*). (*C*) 300 nM of GaMF1 analog **8** increase the potency of (±)-5307 in ATP synthesis inhibition (Δ) when compared to the inhibitory effect of (±)-5307 alone (▲). (*D*) Addition of 500 nM (▲) and 9 µM (■) of GaMF1 analog **8** shifted the inhibition curve to the left, showing a 2-fold (0.7 nM) and 10-fold (0.17 nM) decrease in MIC_{50} thereby revealing the synergistic effect on the same target enzyme. The effect of racemate ((±)-5307) on growth of *M. smegmatis* mc^2 155 is shown in curve (●).

Table 1: SAR of selected GaMF1 analogs

Cpd No.	Structure	IC_{50} (μm)[a]	MIC_{50} (μM)[b]	MIC_{50} (μM)[c]
GaMF1	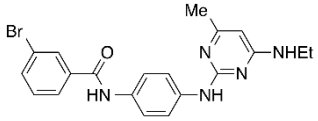	0.5	11	33
1	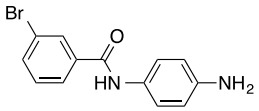	>100	>100	-
2	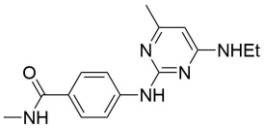	>100	-	-
3	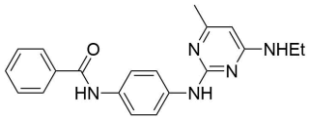	1.7	27	-
4	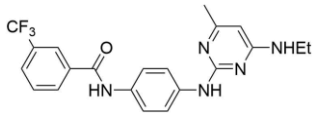	0.23	13.4	10.1
5	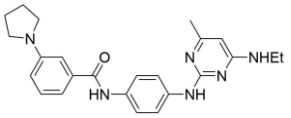	0.21	9.7	13.9
6	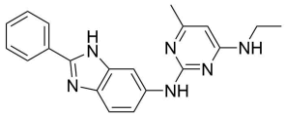	0.28	23.5	8.8
7	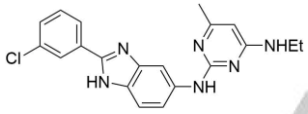	0.29	14.6	5.2
8	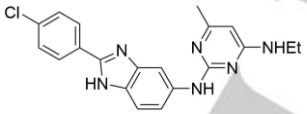	0.09	9.9	3

[a] ATP synthesis Inhibitory Concentration on *M. smegmatis* IMVs
[b] *M. smegmatis* Minimum Inhibitory Concentration
[c] *M. tuberculosis* Minimum Inhibitory Concentration

In an attempt to retain the key amide functionality while addressing potential concerns about toxicity arising due to oxidation of the 1,4-phenylenediamine moiety (ring B), analogs (**6** – **8**) bearing a central benzimidazole motif with a phenyl substituent were synthesized. Such a modification would restrict rotational freedom between the A and B ring while retaining the phenyl substituent. All three analogs displayed good IC_{50} and MIC_{50} values, with one (**8**) showing a 10-fold improvement compared to the original compound, GaMF1. The *p*-chloro phenyl derivative **8** afforded a 18-fold enhancement in ATP synthesis inhibition of about 90 nM on *M. smegmatis* (Fig. 7A) and even 8.7 nM on *M. bovis* BCG IMVs (Fig. 7B) and inhibited *Mtb* growth culture at a concentration of 3 μM, while the *m*-chloro phenyl derivative **7** maintained an activity profile similar to the parent molecule. Interestingly, when 300 nM of analog **8** was combined in an ATP synthesis assay of *M. smegmatis* with (±)-5307 (Fig. 7C) a clear synergistic effect could be observed, reflecting the potency of this unique TB-compound combination. Addition of GaMF1 analog **8** shifted the growth curve to the left, thereby revealing the synergistic effect on the same target enzyme (Fig. 7D).

Conclusion

Respiration is a promising target for the development of new antimycobacterial agents, including the inhibitors clofazimine, Telacebec (Q203), and BDQ which inhibit the mycobacterial complex II (Ndh2; [24]), the cytochrome *bc1* complex [25], and the F-ATP synthase.[3] The latter was approved by FDA for the treatment of MDR-TB in 2012. [4a] An increased understanding of the function and structure of different respiratory complexes and F-ATP synthase in mycobacterial biology is becoming key to advancing cellular bioenergetics as a new target space. [11-13, 14a, 26] Here, we identified a novel TB-compound GaMF1 targeting the unique mycobacterial F-ATP synthase γ-loop and being specific. It retained ATP synthesis inhibition against a BDQ resistant mutant and killing potency against H- and R monoresistant *Mtb* strains as well as the HR-resistant *Mtb* strains. NMR- and docking results of GaMF1 support the mode of action, describing that binding of the compound to the mycobacterial γ-loop interferes with the smooth rotation of the γ subunit along the loop residues of the rotating *c*-ring turbine, thereby interrupting proper coupling of proton conduction in the *a*-*c* subunits and ATP synthesis in the α_3:β_3 headpiece via the central stalk subunit γ. In comparison, BDQ, TBAJ-876 and its derivatives 5307, 5316 and 5377 bind to both subunit *c* [14b] and ε [6d, 14d, 27], and drug binding presumably results in stalling of *c*-ring rotation relative to subunit *a*. [14b] Combining GaMF1 with BDQ or (±)-5307 increased the MIC- and IC potency, while not affecting viability and pluripotency of human embryonic stem cells, which is essential for further clinical applications. Medicinal chemistry efforts resulted in GaMF1 derivatives with increased potency regarding ATP synthesis inhibition and *Mtb* cell viability. Future studies will focus on the utility of the new lead for the treatment of TB, considering that in patients, *Mtb* grows extra- as well as intra-cellular. Here, we demonstrated activity of GaMF1 against *Mtb* growing in broth, i.e. against the extracellular form of the bacterium. Therefore, activity of the new F-ATP synthase inhibitor against intracellular *Mtb* will be determined in macrophage infection models.

Acknowledgements

This research was supported by the National Research Foundation (NRF) Singapore, NRF Competitive Research Programme (CRP), Grant Award Number NRF–CRP18–2017–01. A. Hotra is grateful to receive an IGS Premium Scholarship, Institute of Technology in Health and Medicine at NTU, and J. P. Sarathy received a PhD scholarship from the School of Medicine, NUS, Singapore. We thank Dr. Yongxin Li for the X-ray crystallographic structure determinations.

Conflict of Interest

G.G., R.W.B., A.H., T.D., K.P. are inventors on the patent PCT/SG2018/050075, and G.G., R.W.B., P.S.N. are inventors on the patent 10201911205R which are related to the chemical series described in this article.

Keywords: ATP synthesis • Bioenergetics • Drug Discovery • F-ATP synthase • OXPHOS • Tuberculosis

References

[1] World Health Organization (2019) Global tuberculosis report 2019. *https://www.who.int/tb/publications/global_report/en/*.

[2] a) G. M. Cook, K. Hards, C. Vilcheze, T. Hartman, M. Berney, *Microbiol Spectr* **2014**, *2* doi: 10.1128/microbiolspec; b) S. P. Rao, S. Alonso, L. Rand, T. Dick, K. Pethe, *Proc Natl Acad Sci U S A* **2008**, *105*, 11945-11950.

[3] K. Andries, P. Verhasselt, J. Guillemont, H. W. Gohlmann, J. M. Neefs, H. Winkler, J. Van Gestel, P. Timmerman, M. Zhu, E. Lee, P. Williams, D. de Chaffoy, E. Huitric, S. Hoffner, E. Cambau, C. Truffot-Pernot, N. Lounis, V. Jarlier, *Science* **2005**, *307*, 223-227.

[4] a) K. Andries, C. Villellas, N. Coeck, K. Thys, T. Gevers, L. Vranckx, N. Lounis, B. C. de Jong, A. Koul, *PLoS One* **2014**, *9*, e102135; b) R. C. Hartkoorn, S. Uplekar, S. T. Cole, *Antimicrob Agents Chemother* **2014**, *58*, 2979-2981.

[5] a) A. H. Diacon, P. R. Donald, A. Pym, M. Grobusch, R. F. Patientia, R. Mahanyele, N. Bantubani, R. Narasimooloo, T. De Marez, R. van Heeswijk, N. Lounis, P. Meyvisch, K. Andries, D. F. McNeeley, *Antimicrob Agents Chemother* **2012**, *56*, 3271-3276; b) J. Guillemont, C. Meyer, A. Poncelet, X. Bourdrez, K. Andries, *Future medicinal chemistry* **2011**, *3*, 1345-1360; cFDA, **2012**.

[6] a) A. S. T. Tong, P. J. Choi, A. Blaser, H. S. Sutherland, S. K. Y. Tsang, J. Guillemont, M. Motte, C. B. Cooper, K. Andries, W. Van den Broeck, S. G. Franzblau, A. M. Upton, W. A. Denny, B. D. Palmer, D. Conole, *ACS Med Chem Lett* **2017**, *8*, 1019-1024; b) P. J. Choi, H. S. Sutherland, A. S. T. Tong, A. Blaser, S. G. Franzblau, C. B. Cooper, M. U. Lotlikar, A. M. Upton, J. Guillemont, M. Motte, L. Queguiner, K. Andries, W. Van den Broeck, W. A. Denny, B. D. Palmer, *Bioorg Med Chem Lett* **2017**, *27*, 5190-5196; c) H. S. Sutherland, A. S. T. Tong, P. J. Choi, D. Conole, A. Blaser, S. G. Franzblau, C. B. Cooper, A. M. Upton, M. U. Lotlikar, W. A. Denny, B. D. Palmer, *Bioorganic & medicinal chemistry* **2018**, *26*, 1797-1809; d) J. P. Sarathy, P. Ragunathan, J. Shin, C. B. Cooper, A. M. Upton, G. Grüber, T. Dick, *Antimicrob Agents Chemother* **2019**, *63* pii: e01191-19.

[7] S. J. Tantry, S. D. Markad, V. Shinde, J. Bhat, G. Balakrishnan, A. K. Gupta, A. Ambady, A. Raichurkar, C. Kedari, S. Sharma, N. V. Mudugal, A. Narayan, C. N. Naveen Kumar, R. Nanduri, S. Bharath, J. Reddy, V. Panduga, K. R. Prabhakar, K. Kandaswamy, R. Saralaya, P. Kaur, N. Dinesh, S. Guptha, K. Rich, D. Murray, H. Plant, M. Preston, H. Ashton, D. Plant, J. Walsh, P. Alcock, K. Naylor, M. Collier, J. Whiteaker, R. E. McLaughlin, M. Mallya, M. Panda, S. Rudrapatna, V. Ramachandran, R. Shandil, V. K. Sambandamurthy, K. Mdluli, C. B. Cooper, H. Rubin, T. Yano, P. Iyer, S. Narayanan, S. Kavanagh, K. Mukherjee, V. Balasubramanian, V. P. Hosagrahara, S. Solapure, S. Ravishankar, P. S. Hameed, *J Med Chem* **2017**, *60*, 1379-1399.

[8] S. Kumar, R. Mehra, S. Sharma, N. P. Bokolia, D. Raina, A. Nargotra, P. P. Singh, I. A. Khan, *Tuberculosis* **2018**, *108*, 56-63.

[9] W. G. Saw, M. L. Wu, P. Ragunathan, G. Biuković, A. M. Lau, J. Shin, A. Harikishore, C. Y. Cheung, K. Hards, J. P. Sarathy, R. W. Bates, G. M. Cook, T. Dick, G. Grüber, *Scientific Rep.* **2019**, *9*, 16759.

[10] a) A. Mandavilli, *Nature medicine* **2007**, *13*, 271; b) D. G. Russell, C. E. Barry, 3rd, J. L. Flynn, *Science* **2010**, *328*, 852-856.

[11] A. Koul, E. Arnoult, N. Lounis, J. Guillemont, K. Andries, *Nature* **2011**, *469*, 483-490.

[12] C. M. Sassetti, D. H. Boyd, E. J. Rubin, *Mol Microbiol* **2003**, *48*, 77-84.

[13] G. M. Cook, K. Hards, E. Dunn, A. Heikal, Y. Nakatani, C. Greening, D. C. Crick, F. L. Fontes, K. Pethe, E. Hasenoehrl, M. Berney, *Microbiol Spectr* **2017**, *5*.

[14] a) A. T. Zhang, M. G. Montgomery, A. G. W. Leslie, G. M. Cook, J. E. Walker, *Proc Natl Acad Sci U S A* **2019**; b) L. Preiss, J. D. Langer, O. Yildiz, L. Eckhardt-Strelau, J. E. Guillemont, A. Koul, T. Meier, *Sci Adv* **2015**, *1*, e1500106; c) N. Kamariah, R. G. Huber, W. Nartey, S. Bhushan, P. J. Bond, G. Grüber, *J Struct Biol* **2019**, *207*, 199-208; d) S. Joon, P. Ragunathan, L. Sundararaman, W. Nartey, S. Kundu, M. S. S. Manimekalai, N. Bogdanović, T. Dick, G. Grüber, *FEBS J* **2018**, *285*, 1111-1128; e) N. Kamariah, P. Ragunathan, J. Shin, W. G. Saw, C. F. Wong, T. Dick, G. Grüber, *Progr. Biophysi. Mol. Biol.* **2019**, 152, 64-73.

[15] A. Hotra, M. Suter, G. Biuković, P. Ragunathan, S. Kundu, T. Dick, G. Grüber, *FEBS J* **2016**, *283*, 1947-1961.

[16] R. Priya, G. Biuković, M. S. Manimekalai, J. Lim, S. P. Rao, G. Grüber, *J Bioenerg Biomembr* **2013**, *45*, 121-129.

[17] A. Koul, L. Vranckx, N. Dhar, H. W. Gohlmann, E. Ozdemir, J. M. Neefs, M. Schulz, P. Lu, E. Mortz, J. D. McKinney, K. Andries, D. Bald, *Nat Commun* **2014**, *5*, 3369.

[18] P. Ragunathan, H. Sielaff, L. Sundararaman, G. Biuković, M. S. Subramanian Manimekalai, D. Singh, S. Kundu, T. Wohland, W. Frasch, T. Dick, G. Grüber, *J Biol Chem* **2017**, *292*, 11262-11279.

[19] N. P. Kalia, E. J. Hasenoehrl, N. B. Ab Rahman, V. H. Koh, M. L. T. Ang, D. R. Sajorda, K. Hards, G. Grüber, S. Alonso, G. M. Cook, M. Berney, K. Pethe, *Proc Natl Acad Sci U S A* **2017**, *114*, 7426-7431.

[20] a) S. Petrella, E. Cambau, A. Chauffour, K. Andries, V. Jarlier, W. Sougakoff, *Antimicrob Agents Chemother* **2006**, *50*, 2853-2856; b) S. Kundu, G. Biuković, G. Grüber, T. Dick, *Antimicrob Agents Chemother* **2016**, *60*, 6977-6979.

[21] R. C. Hartkoorn, S. Uplekar, S. T. Cole, Antimicrob Agents Chemother **2014**, *58*, 2979-2981.

[22] a) K. G. Chen, B. S. Mallon, K. Park, P. G. Robey, R. D. G. McKay, M. M. Gottesman, W. Zheng, *Trends in molecular medicine* **2018**, *24*, 805-820; b) Y. Avior, I. Sagi, N. Benvenisty, *Nature reviews. Molecular cell biology* **2016**, *17*, 170-182.

[23] S. H. Vijaya Chandra, H. Makhija, S. Peter, C. M. Myint Wai, J. Li, J. Zhu, Z. Ren, M. S. D'Alcontres, J. W. Siau, S. Chee, F. J. Ghadessy, P. Dröge, *Nucleic Acids Res* **2016**, *44*, e55.

[24] T. Yano, S. Kassovska-Bratinova, J. S. Teh, J. Winkler, K. Sullivan, A. Isaacs, N. M. Schechter, H. Rubin, *J Biol Chem* **2011**, *286*, 10276-10287.

[25] K. Pethe, P. Bifani, J. Jang, S. Kang, S. Park, S. Ahn, J. Jiricek, J. Jung, H. K. Jeon, J. Cechetto, T. Christophe, H. Lee, M. Kempf, M. Jackson, A. J. Lenaerts, H. Pham, V. Jones, M. J. Seo, Y. M. Kim, M. Seo, J. J. Seo, D. Park, Y. Ko, I. Choi, R. Kim, S. Y. Kim, S. Lim, S. A. Yim, J. Nam, H. Kang, H. Kwon, C. T. Oh, Y. Cho, Y. Jang, J. Kim, A. Chua, B. H. Tan, M. B. Nanjundappa, S. P. Rao, W. S. Barnes, R. Wintjens, J. R. Walker, S. Alonso, S. Lee, J. Kim, S. Oh, T. Oh, U. Nehrbass, S. J. Han, Z. No, J. Lee, P. Brodin, S. N. Cho, K. Nam, J. Kim, *Nature medicine* **2013**, *19*, 1157-1160.

[26] a) B. Wiseman, R. G. Nitharwal, O. Fedotovskaya, J. Schafer, H. Guo, Q. Kuang, S. Benlekbir, D. Sjostrand, P. Adelroth, J. L. Rubinstein, P. Brzezinski, M. Hogbom, *Nat Struct Mol Biol* **2018**, *25*, 1128-1136; b) H. Gong, J. Li, A. Xu, Y. Tang, W. Ji, R. Gao, S. Wang, L. Yu, C. Tian, J. Li, H. Y. Yen, S. Man Lam, G. Shui, X. Yang, Y. Sun, X. Li, M. Jia, C. Yang, B. Jiang, Z. Lou, C. V. Robinson, L. L. Wong, L. W. Guddat, F. Sun, Q. Wang, Z. Rao, *Science* **2018**, *362*; c) W. Moreira, D. B. Aziz, T. Dick, *Frontiers in microbiology* **2016**, *7*, 199.

[27] G. Biuković, S. Basak, M. S. Manimekalai, S. Rishikesan, M. Roessle, T. Dick, S. P. Rao, C. Hunke, G. Grüber, *Antimicrob Agents Chemother* **2013**, *57*, 168-176.

Entry for the Table of Contents

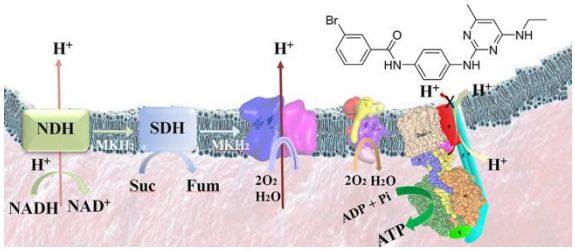

The antimycobacterial GaMF1 inhibits the mycobacterial F-ATP synthase by binding to a specific loop of subunit γ, preventing ATP synthesis via oxidative phosphorylation. The bactericidal compound is active against multidrug-resistant strains, increased the potency of the TB-drug Bedaquiline and other DARQ analogues, opening a new avenue for an efficient multi-drug combination. Chemistry efforts resulted in analogues with nanomolar potencies.